MR Imaging and Spectroscopy for evaluation of brain tumor metabolic profiles in primary glioblastoma multiforme xenografts

Yanping Sun[1], Matthew C Dunn[1], Saadallah Ramadan[2], Kristen L Jones[1], Adam Green[3], Keith Ligon[4], and Andrew L Kung[1,5]

[1]Lurie Family Imaging Center, Dana Farber Cancer Institute, Harvard Medical School, Boston, MA, United States, [2]School of Health Sciences, University of Newcastle, Callaghan, NSW, Australia, [3]Pediatric Oncology, Dana Farber Cancer Institute, Harvard Medical School, Boston, MA, United States, [4]Medical Oncology, Dana Farber Cancer Institute, Harvard Medical School, Boston, MA, United States, [5]Pediatric Hematology/ Oncology/Stem Cell Transplantation, Columbia University Medical Center, New York, NY, United States

Introduction: Malignant brain tumors generally develop rapidly to a fatal stage with a median survival of 12 months. More effective treatments are urgently needed. To evaluate the effects of drug candidates for brain tumors, a clinically faithful animal model is essential. Cell line xenografts, utilizing cell lines such as U87-MG, generally do not recapitulate clinical characteristics such as infiltrative growth. In contrast, direct inoculation of surgical resection material, so called primary xenograft tumor models, often more closely replicating clinical disease. We used multimodality imaging to characterize an orthotopic (intracranial) glioblastoma multiforme (GBM) primary xenograft model. Bioluminescence imaging (BLI) was used to monitor tumor growth. MRI and MR spectroscopy (MRS) were used to evaluate the tumor metabolic properties.

Methods: A primary human GBM line, BT145, was lentivirally transduced with a Luc-mCherry-puro virus to generate BT145-mCLP cells. BT145-mCLP cells (180,000 in 1 µl) were stereotactically injected in the right striatum of nude mice. BLI was performed using an IVIS Spectrum system (Caliper Life Sciences) to monitor tumor growth. Peak total tumor BLI signal through standardized regions of interest (ROI) were calculated using the Living Images software package (version 4.0, Caliper Life Sciences), with data presented as total flux in photons per second per ROI. When the BLI signal of tumors reached $2x10^8$ ph/s/cm^2/sr, MRI and MRS were conducted (n=5). The MR experiments were carried out on a Bruker 7T MRI system. Mice were anesthetized with 1-1.5% isoflurane in medical air. T2 weighted images with RARE sequence were acquired for tumor visualization. T1, T2 and diffusion measurements were acquired for characterization of the BT145 tumor using IR, MSME and EPI-SpinEcho diffusion methods. MRS was acquired from the tumor region (right hemisphere) and the contralateral region in the brain using point resolved spectroscopy (PRESS) method with TR=4000ms, TE= 7ms, number of points=4096, average of 512, cube size =3x3x3mm. MRS data was analyzed using Bruker TopSpin analysis tool and JMRUI (v4) using HLSVD approach (Hankel Lanczos Squares Singular Values Decomposition**,** 15 components, 2k points in HLSVD, Hankel Matrix points 1k, with Lancoz approach implemented (1)).

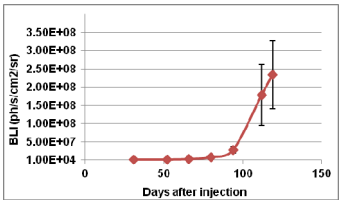

Fig.1. Tumor growth curve by BLI.

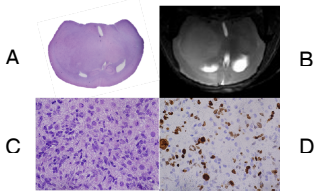

Fig.2. Comparison of MRI and histologic findings

Results: Fig. 1 demonstrates the growth of the BT145 tumors over time by BLI measurement. On week 17 after the tumor injection, the average BLI was $2.3x10^8 \pm 9.4 x10^7$ ph/s/cm^2/sr. Fig.2 demonstrates the correlation between histopathology and MRI imaging of BT145 xenografts. A coronal brain section (H&E) of the BT145 xenograft (Fig. A) shows a diffusely infiltrating neoplasm predominantly involving the right hemisphere with ventricular compression and midline shift, which is consistent with the pattern observed by MRI (Fig. B). At 60x magnification (Fig. C), the tumor is characterized as a densely cellular high-grade glioma, with a high percentage of proliferating cells, indicated by positive immunohistochemistry to Ki-67 (Fig. D). Table 1 shows the T1, T2 and ADC values in tumor were significantly higher than those in contralateral brain tissue. The 5 tumor spectra and 5 contralateral spectra were summed respectively to yield one spectrum in each case as shown in Fig. 3. Major metabolites were identified with corresponding peaks; the ratios of detected metabolites to Cr were calculated and plotted for both groups in Fig 4. Major metabolites that were shown to change are also shown in Fig 4. The ratios of NAA, GABA, Cho, Tryp/Glc/myo-ino, Cho/myo-ino/Tryp to Cr in tumors were significantly different compared to those in contralateral brain tissue. These metabolic peaks were indicated with black arrows in Fig. 3. The Cho/NAA statistical index (CNI) was significantly higher in tumor (CNI=4.3) than in control tissue (CNI=1.4).

Table 1. T1, T2 and ADC values

	T1 (ms)	T2 (ms)	ADC($x10^{-3}$ mm^2 s^{-1})
Tumor	1901±164	63±4	0.70 ±0.068
Contralateral	1612±47	46±2	0.53±0.097
P-value	0.005	1.65E-05	0.01

Discussion and Conclusions: In this study, we demonstrate that in this primary GBM xenograft model, tumor tissue had higher T1, T2 and diffusion values by comparison to the contralateral region in the brain, consistent with GBM in human patients (2). MRS assessment of the metabolic profile of the primary GBM xenografts revealed a reduction of NAA and GABA, and elevation of Lipid, Cho, Myo, Glx in tumors, which is likewise in agreement with prior human MRS GBM studies (3). Moreover, histologic analysis revealed an infiltrative pattern of growth, similar to disease in humans. Together, these results demonstrate that this primary xenograft model of GBM closely recapitulates the histological, radiologic and metabolic profile of human GBM.

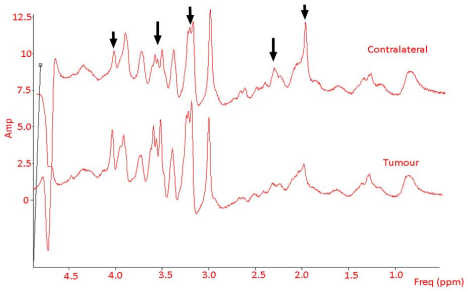

Fig.3. Comparison of average spectra from tumor and contralateral sides of mouse brain. Five spectra were summed up in each case.

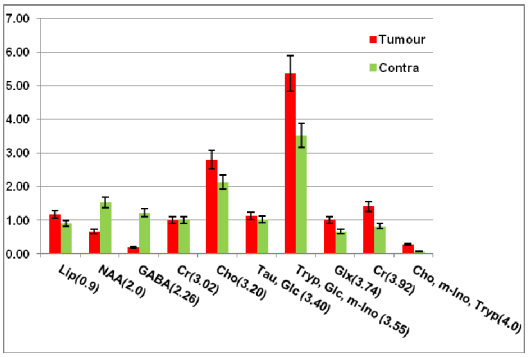

Fig 4. Comparison of metabolite integral ratio to Cr of major metabolites in tumor and contralateral sides identified by MRS. 10% error was added to all values.

References : [1]Pijnappel, et al, J. Magn.Reson(1992); 97:122. [2]Yamasaki, et al, Radiology (2005); 235, 985-991. [3] Ramadan, et al, Radiology(2011); 259: 540-549